Forward jet production at the Large Hadron Collider

JHEP09(2009)121

(http://iopscience.iop.org/1126-6708/2009/09/121)

Published by IOP Publishing for SISSA

Received: *August 5, 2009*
Accepted: *September 4, 2009*
Published: *September 29, 2009*

Forward jet production at the Large Hadron Collider

M. Deak,[a] **F. Hautmann,**[b] **H. Jung**[a] **and K. Kutak**[a]

[a] *Deutsches Elektronen Synchrotron, D-22603 Hamburg, Germany*
[b] *Theoretical Physics, University of Oxford, Oxford OX1 3NP, U.K.*
E-mail: mideak@mail.desy.de, hautmann@thphys.ox.ac.uk, jung@mail.desy.de, kutak@mail.desy.de

Abstract: At the Large Hadron Collider (LHC) it will become possible for the first time to investigate experimentally the forward region in hadron-hadron collisions via high-p_T processes. In the LHC forward kinematics QCD logarithmic corrections in the hard transverse momentum and in the large rapidity interval may both be quantitatively significant. We analyze the hadroproduction of forward jets in the framework of QCD high-energy factorization, which allows one to resum consistently both kinds of corrections to higher orders in QCD perturbation theory. We compute the short-distance matrix elements needed to evaluate the factorization formula at fully exclusive level. We discuss numerically dynamical features of multi-gluon emission at large angle encoded in the factorizing high-energy amplitudes.

Keywords: Jets, Hadronic Colliders, QCD

ArXiv ePrint: 0908.0538

doi:10.1088/1126-6708/2009/09/121

JHEP09(2009)121

Contents

JHEP09(2009)121

1 Introduction

Experiments at the Large Hadron Collider (LHC) will explore the region of large rapidities both with general-purpose detectors and with dedicated instrumentation, including forward calorimeters and proton taggers [1–7]. The forward-physics program involves a wide range of topics, from new particle discovery processes [3, 8, 9] to new aspects of strong interaction physics [7, 10, 11] to heavy-ion collisions [12, 13]. Owing to the large center-of-mass energy and the unprecedented experimental coverage at large rapidities, it becomes possible for the first time to investigate the forward region with high-p_T probes.

The hadroproduction of a forward jet associated with a hard final state X is pictured in figure 1. The kinematics of the process is characterized by the large ratio of sub-energies $s_1/s \gg 1$ and highly asymmetric longitudinal momenta in the partonic initial state, $k_1 \cdot p_2 \gg k_2 \cdot p_1$. At the LHC the use of forward calorimeters allows one to measure events where jet transverse momenta $p_T > 20\,\text{GeV}$ are produced several units of rapidity apart, $\Delta y \gtrsim 4 \div 6$ [1, 5, 7]. Working at polar angles that are small but sufficiently far from the beam axis not to be affected by beam remnants, one measures azimuthal plane correlations between high-p_T events widely separated in rapidity (figure 2).

The presence of multiple large-momentum scales implies that, as was recognized in [14–16], reliable theoretical predictions for forward jets can only be obtained after summing logarithmic QCD corrections at high energy to all orders in α_s. This has motivated efforts [17–20] to construct new algorithms for Monte Carlo event generators capable of describing jet production beyond the central rapidity region. Note that an analogous observation applies to forward jets associated to deeply inelastic scattering [21, 22]. Indeed, measurements of forward jet cross sections at HERA [23] indicate that neither fixed-order next-to-leading calculations nor standard shower Monte Carlo generators [17, 23, 24], e.g. Pythia or Herwig, are able to describe forward jet ep data. Improved methods to evaluate QCD predictions are needed to treat the multi-scale region implied by the forward kinematics.

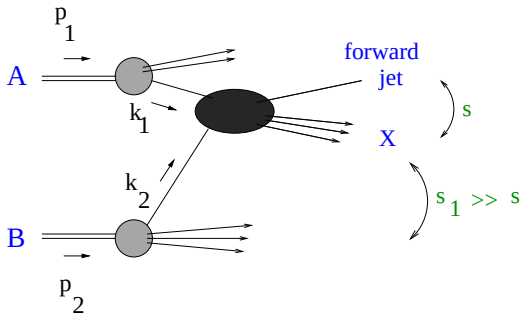

Figure 1. Jet production in the forward rapidity region in hadron-hadron collisions.

Figure 2. (Left) High-p_T events in the forward and central detectors; (right) azimuthal plane segmentation.

In this work we move on from the observation that realistic phenomenology in the LHC forward region will require taking into account at higher order both logarithmic corrections in the large rapidity interval (of high-energy type) and logarithmic corrections in the hard transverse momentum (of collinear type). The theoretical framework to resum consistently both kinds of logarithmic corrections in QCD perturbation theory is based on high-energy factorization at fixed transverse momentum [25].

This formulation depends on unintegrated distributions for parton splitting, obeying appropriate evolution equations, and short-distance, process-dependent matrix elements. The unintegrated-level evolution is given by evolution equations in rapidity, or angle, parameters. Different forms of the evolution, valid in different kinematic regions, are available. See [26–29], and references therein, for recent work in this area and reviews. The short-distance matrix elements, needed in the evaluation of the factorization formula, are the subject of this paper. We obtain their explicit expressions in a fully exclusive form, including all partonic channels, and present results of numerically integrating them over final states. Such matrix elements, though not on shell, are gauge invariant and perturbatively calculable. They factorize in the high energy limit in front of (unintegrated) distributions for parton splitting not only in the collinear emission region but also at finite angle. In particular, they can serve to take into account effects of coherence from multi-gluon emission, away from small angles, which become important for correlations among jets across long separations in rapidity. We give a numerical illustration of the high-k_T behavior resulting from such finite-angle radiation.

On one hand, once convoluted with the small-x gluon Green's function according to the method [25, 30], these matrix elements control the summation of high-energy logarithmic corrections, contributing both to the next-to-leading-order BFKL kernel [31] and to the jet impact factors [32, 33]. On the other hand, they can be used in a shower Monte Carlo implementing parton-branching kernels at unintegrated level (see e.g. [34, 35] for recent works) to generate fully exclusive events. We leave these applications to a separate paper.

JHEP09(2009)121

The paper is organized as follows. After recalling the factorized form of the cross sections in section 2, we present the high-energy amplitudes in section 3, and discuss basic properties and numerical results in section 4. We summarize in section 5.

2 High-energy factorized cross sections

High-energy factorization [25] allows one to decompose the cross section for the process of figure 1 into partonic distributions (in general, unintegrated) and hard-scattering kernels, obtained via the high-energy projectors [25, 30] from the amplitudes for the process $p_1 + p_2 \to p_3 + p_4 + 2$ massless partons. The basic structure is depicted in figure 3.

With reference to the notation of figure 3, let us work in the center of mass frame of the incoming momenta

$$p_1 = \sqrt{S/2}(1, 0, 0_T) \quad , \qquad p_2 = \sqrt{S/2}(0, 1, 0_T) \quad , \qquad 2p_1 \cdot p_2 = S \quad , \tag{2.1}$$

where, for any four-vector, $p^\mu = (p^+, p^-, p_T)$, with $p^\pm = (p^0 \pm p^3)/\sqrt{2}$ and p_T two-dimensional euclidean vector. Let us parameterize the exchanged momenta in terms of purely transverse four-vectors $k_\perp$ and $k_{\perp 1}$ and longitudinal momentum fractions ξ_i and $\overline{\xi}_i$ as

$$p_1 - p_5 = k_1 = \xi_1 p_1 + k_{\perp 1} + \overline{\xi}_1 p_2 \quad , \quad p_2 - p_6 = k_2 = \xi_2 p_2 + k_\perp + \overline{\xi}_2 p_1 \quad . \tag{2.2}$$

For high energies we can introduce strong ordering in the longitudinal momenta, $\xi_1 \gg |\overline{\xi}_2|$, $\xi_2 \gg |\overline{\xi}_1|$. Further, we make the forward region approximations $(p_4 + p_6)^2 \gg (p_3 + p_4)^2$, $k_1 \simeq \xi_1 p_1$, $k_2 \simeq \xi_2 p_2 + k_\perp$, so that

$$p_5 \simeq (1 - \xi_1) p_1 \quad , \quad p_6 \simeq (1 - \xi_2) p_2 - k_\perp \quad , \quad \xi_1 \gg \xi_2 \quad . \tag{2.3}$$

It is convenient to define the rapidity-weighted average of dijet transverse momenta,

$$Q_T = (1 - \nu) p_{T4} - \nu p_{T3} \quad , \quad \text{where} \quad \nu = (p_2\, p_4)/[(p_2\, p_1) - (p_2\, p_5)] \quad , \tag{2.4}$$

and the azimuthal angle

$$\cos\varphi = Q_T \cdot k_T / |Q_T||k_T| \quad . \tag{2.5}$$

We consider the differential jet cross section in Q_T and φ.

According to the factorization [25, 32], the jet cross section can be computed as (figure 3a)

$$\frac{d\sigma}{dQ_T^2 d\varphi} = \sum_a \int d\xi_1\, d\xi_2\, d^2k_T\, \phi_{a/A}(\xi_1)\, \frac{d\widehat{\sigma}}{dQ_T^2 d\varphi}(\xi_1\xi_2 S, k_T, Q_T, \varphi)\, \phi_{g^*/B}(\xi_2, k_T) \quad , \tag{2.6}$$

where the sum goes over parton species, ϕ are the parton distributions defined from the unintegrated Green's functions introduced in [30] for both gluon and quark cases, and $\widehat{\sigma}$ is the hard cross section, calculable from the high-energy limit of perturbative amplitudes (figure 3b).

The physical picture underlying eq. (2.6) is based on the fact that initial-state parton configurations contributing to forward production are asymmetric, with the parton in the

JHEP09(2009)121

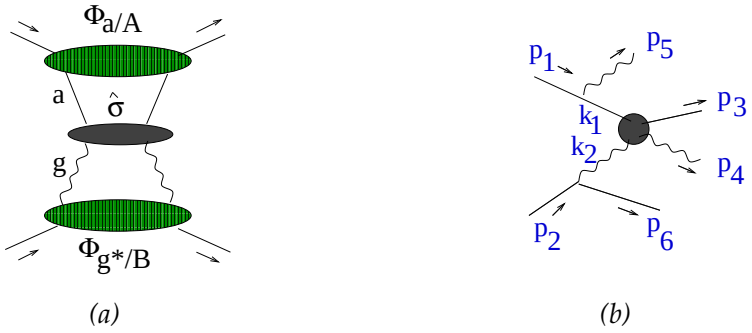

Figure 3. (a) Factorized structure of the cross section; (b) a graph contributing to the qg channel matrix element.

top subgraph being probed near the mass shell and large x, while the parton in the bottom subgraph is off-shell and small-x. Eq. (2.6) embodies this picture through the longitudinal and transverse momentum dependences of both ϕ and $\widehat{\sigma}$.

For phenomenological studies we will be interested in coupling eq. (2.6) to parton showers to achieve a full description of the associated final states. To this end we need the matrix elements defining the hard-scattering kernels in a fully exclusive form. We give the results in the next section.

3 Matrix elements for fully exclusive events

The matrix elements determining the hard-scattering kernels $\widehat{\sigma}$ can be viewed as a suitably defined off-shell continuation of scattering amplitudes at lower order [25]. They can be obtained by applying to scattering amplitudes $\mathcal{M}$ the high-energy eikonal projectors [25, 30],

$$\mathcal{M}^H = P^{H\ \mu_1\mu_2\cdots}_{(eik)}\ \mathcal{M}_{\mu_1\mu_2\cdots}(k_1,k_2,\{p_i\})\ ,\quad P^{H\ \mu_1\mu_2\cdots}_{(eik)} \propto \frac{2k_{\perp 1}^{\mu_1}k_{\perp 2}^{\mu_2}}{\sqrt{k_{\perp 1}^2 k_{\perp 2}^2}}\ . \tag{3.1}$$

Although they are not evaluated on shell, they are gauge invariant and their expressions are simple. The utility of these matrix elements is that in the high-energy limit they factorize not only in the collinear emission region but also in the large-angle emission region. As long as the factorization is carried out in terms of distributions for parton splitting at fixed transverse momentum, as in eq. (2.6), they can be useful to include coherence effects [32] from multi-gluon emission across large rapidity intervals, not associated with small angles.

The results for the matrix elements in exclusive form are given by

$$\mathcal{M}_{qg\to qg} = C_1\mathcal{A}_1^{(ab)} + \overline{C}_1\mathcal{A}_1^{(nab)}\ ,\quad \mathcal{M}_{gg\to q\overline{q}} = C_2\mathcal{A}_2^{(ab)} + \overline{C}_2\mathcal{A}_2^{(nab)}\ ,\quad \mathcal{M}_{gg\to gg} = C_3\mathcal{A}_3 \tag{3.2}$$

where

$$\mathcal{A}_1^{(ab)} = \left(\frac{k_1k_2}{k_1p_2}\right)^2 \frac{(k_1p_2)^2+(p_2p_3)^2}{(k_1p_4)(p_3p_4)}\ , \tag{3.3}$$

$$\mathcal{A}_1^{(nab)} = \left(\frac{k_1k_2}{k_1p_2}\right)^2 \frac{(k_1p_2)^2+(p_2p_3)^2}{(k_1p_4)(p_3p_4)}\left(\frac{(p_3p_4)(k_1p_2)}{(k_1p_3)(p_2p_4)} + \frac{(k_1p_4)(p_2p_3)}{(k_1p_3)(p_2p_4)} - 1\right)\ , \tag{3.4}$$

JHEP09(2009)121

$$\mathcal{A}_2^{(ab)} = \left(\frac{k_1k_2}{k_1p_2}\right)^2 \frac{(p_2p_3)^2+(p_2p_4)^2}{(k_1p_4)(k_1p_3)}\,, \tag{3.5}$$

$$\mathcal{A}_2^{(nab)} = \left(\frac{k_1k_2}{k_1p_2}\right)^2 \frac{(p_2p_3)^2+(p_2p_4)^2}{(k_1p_4)(k_1p_3)} \left(\frac{(k_1p_4)(p_2p_3)}{(p_3p_4)(k_1p_2)} + \frac{(k_1p_3)(p_2p_4)}{(p_3p_4)(k_1p_2)} - 1\right)\,, \tag{3.6}$$

$$\mathcal{A}_3 = \left(\frac{k_1k_2}{k_1p_2}\right)^2 \frac{(p_3p_4)(k_1p_2)+(k_1p_4)(p_2p_3)+(p_2p_4)(k_1p_3)}{(p_2p_4)(k_1p_4)(p_3p_4)(k_1p_2)(p_2p_3)(k_1p_3)} \left[(p_2p_4)^4+(k_1p_2)^4+(p_2p_3)^4\right]\,, \tag{3.7}$$

and $C_1 = g^4(N_c^2-1)/(4N_c^2)$, $\overline{C}_1 = C_1C_A/(2C_F)$, $C_2 = g^4/(2N_c)$, $\overline{C}_2 = C_2C_A/(2C_F)$, $C_3 = g^4N_c^2/(N_c^2-1)$.

The results above contain the dependence on the transverse momentum $\mathrm{k}_\perp$ along the parton lines that connect the hard scatter to the parton distributions. Nevertheless, they are short-distance in the sense that they can be safely integrated down to $\mathrm{k}_\perp = 0$. That is, the high-energy projection is designed so that all infrared contributions are factored out in the nonperturbative Green's functions ϕ in eq. (2.6). An explicit numerical illustration is given in the next section.[1]

The role of eqs. (3.3)–(3.7) is twofold. On one hand, they give the high-energy limit of multi-parton matrix elements in the forward region, which may be of direct phenomenological significance. On the other hand, because of the factorization theorem [25], logarithmically enhanced corrections for large rapidity can be systematically obtained to all orders in α_s from those in the (unintegrated) distributions for parton splitting once the hard scattering functions are known at finite $\mathrm{k}_\perp$. To this end the detailed form of the fall-off at large $|\mathrm{k}_\perp|^2$ is relevant.

In the next section we discuss the behavior at high transverse momentum numerically. This behavior reflects properties of gluon emission at large angle encoded in the high-energy amplitudes. These are relevant, along with large-angle effects in the Sudakov region (see e.g. [37]), to achieve a full treatment of gluon coherence effects [38] capable of describing jet final states across the whole rapidity phase space. A uniform treatment of the high-energy and Sudakov regions is still an open issue [39] of interest for parton-shower implementations.

4 Numerical results

We now partially integrate the amplitudes over final states. We work at the level of hard scattering matrix elements, leaving the treatment of parton evolution by showering to a separate study [40]. We concentrate on the region of hard emissions, where jets are well separated. Regions near the boundary of the angular phase space are sensitive to infrared radiation and can be addressed within a full parton-shower description of the process.

[1] Although the hard-scattering functions constructed from the amplitudes in eqs. (3.3)–(3.7) are not coefficient functions in the conventional sense of the operator product expansion, they can be related to such objects, for inclusive variables, along the lines e.g. of [30]. They could be interpreted in terms of coefficient functions in the sense of the high-energy OPE of [36].

JHEP09(2009)121

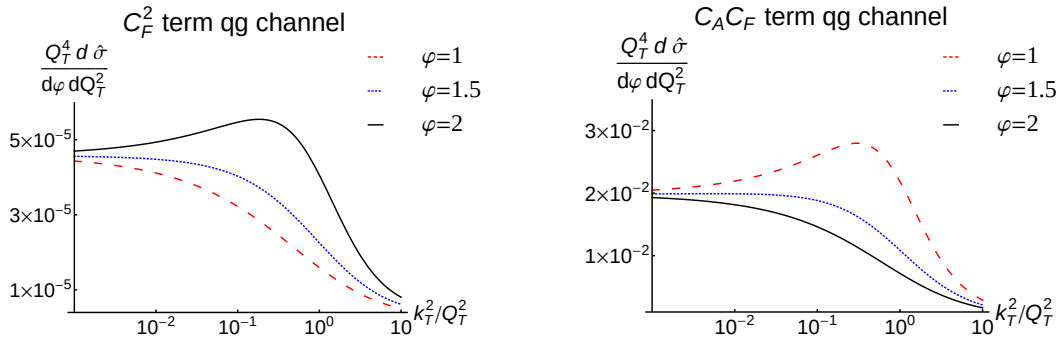

Figure 4. The k_T/Q_T dependence of the factorizing qg hard cross section at high energy: (left) C_F^2 term; (right) $C_F C_A$ term ($\xi_1\xi_2 S/Q_T^2 = 10^2$, $\alpha_s = 0.2$).

We consider the differential distribution in the transverse variable Q_T and azimuthal angle φ. The variable Q_T describes the imbalance in transverse momentum between the hardest jets, weighted by ν, according to eq. (2.4). In figures 4 and 5 we show numerical results versus transverse momentum and versus energy (qg channel).

The curves in figure 4 measure the k_T distribution of the jet system recoiling against the leading di-jets. The result at $k_T/Q_T \to 0$ in these plots returns the lowest-order result, i.e., the leading-order process with two back-to-back jets,

$$\frac{d\widehat{\sigma}}{dQ_T^2 d\varphi} \to \alpha_s^2 f^{(0)}(p_T^2/s) \quad , \quad Q_T \to p_T = |p_{T3}| = |p_{T4}| \quad , \tag{4.1}$$

where $s = (p_3 + p_4)^2$, and $f^{(0)}$ is given by

$$f^{(0)}(z) = \frac{1}{16\sqrt{1-4z}} \left[C_F^2 z(1+z) + 2C_F C_A (1 - 3z + z^2) \right] \quad . \tag{4.2}$$

The dependence on k_T and φ plotted in figure 4 is the result of higher-order gluon radiation, treated according to the high-energy asymptotics. The different behaviors in φ for the C_F^2 and $C_A C_F$ terms reflect the fact that the former comes from the insertion of gluons on fermion-exchange amplitude while the latter comes from the insertion of gluons on vector-exchange amplitude.

Figure 5 shows the energy dependence for fixed k_T/Q_T. The constant asymptotic behavior at large s due to color-octet spin-1 exchange distinguishes the $C_F C_A$ term from the C_F^2 term. The dependence on the azimuthal angle in figures 4 and 5 is relevant, especially because forward jet measurements will rely on azimuthal plane correlations between jets far apart in rapidity (figure 2).

While eq. (4.2) gives the collinear emission limit, we see from figure 4 that multi-gluon radiation at finite angles sets a dynamical cut-off at values of k_T of order Q_T,

$$k_T \lesssim \mu = c\, Q_T \quad . \tag{4.3}$$

The physical meaning of this result is that the summation of the higher-order logarithmic corrections for large $y \sim \ln s/p_T^2$ is precisely determined [25, 32] by convoluting the uninte-

JHEP09(2009)121

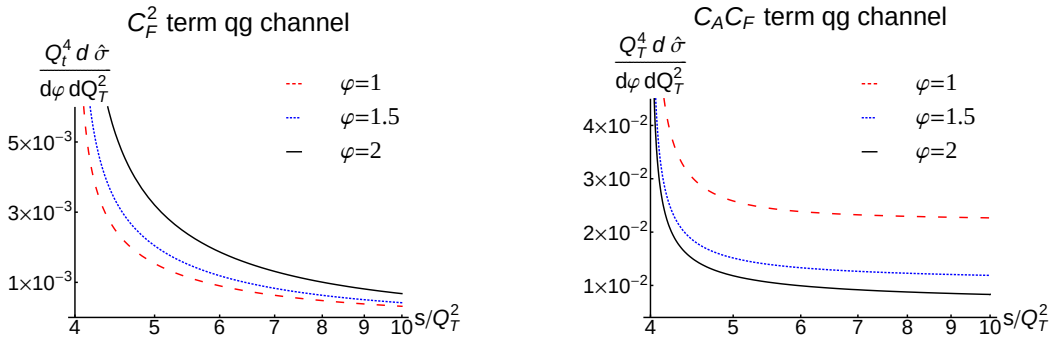

Figure 5. The energy dependence of the qg hard cross section ($k_T/Q_T = 1$).

grated splitting functions over the k_T-dependence in figure 4, via the distributional relation

$$\int d^2k_T \left(\frac{1}{k_T^2}\right)_+ \widehat{\sigma}(k_T) = \int d^2k_T \frac{1}{k_T^2} \left[\widehat{\sigma}(k_T) - \Theta(\mu - k_T)\, \widehat{\sigma}(0_T)\right] \quad . \tag{4.4}$$

So the results in figure 4 illustrate quantitatively the significance of contributions with $k_T \simeq Q_T$ in the large-y region. Non-negligible effects arise at high energy from the finite-k_T tail. These effects are not included in collinear-branching generators (and only partially in fixed-order perturbative calculations), and become more and more important as the jets are observed at large rapidity separations.

Observe that calculations based on the unintegrated formalism will in general depend on two scales, μ and the rapidity, or angle, cut-off [26, 39, 41]. See e.g. the one-loop calculation [29] for an explicit example. It will be of interest to investigate the effect of eq. (4.3) on the behavior in rapidity distributions [40].

Results for gluon-gluon channels are reported in figure 6. Note the large effect of the purely gluonic component. The behavior versus k_T is qualitatively similar to that in figure 4. Calculations in progress [40], including parton showering, indicate that quark and gluon channels give contributions of comparable size in the LHC forward kinematics. The inclusion of both is relevant for realistic studies of phenomenology [11, 42]. Since the forward kinematics selects asymmetric parton momentum fractions, effects due to the $x \to 1$ endpoint behavior [29, 43] at fixed transverse momentum may become phenomenologically significant as well.

We conclude this section by recalling that dynamical effects of high parton densities have been studied [10, 44] as potential contributions to forward jet events. We note that if such effects show up at the LHC, the unintegrated formulation discussed above would likely be the natural framework to implement this dynamics at parton-shower level.

5 Conclusions

Forward + central detectors at the LHC allow jet correlations to be measured across rapidity intervals of several units, $\Delta y \gtrsim 4 \div 6$. Such multi-jet states can be relevant to new particle discovery processes as well as new aspects of standard model physics.

JHEP09(2009)121

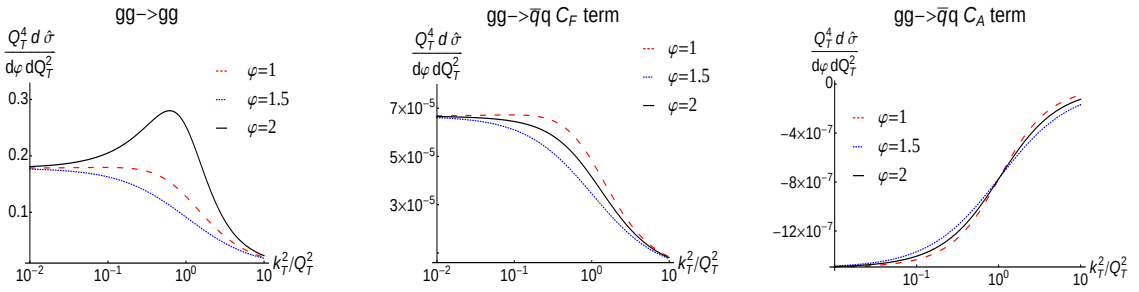

Figure 6. The k_T/Q_T dependence of the factorizing gg matrix elements: (a) $gg \to gg$; (b) $gg \to q\bar{q}$ C_F term; (c) $gg \to q\bar{q}$ C_A term ($\xi_1\xi_2 S/Q_T^2 = 10^2$, $\alpha_s = 0.2$).

Existing sets of forward-jet data in ep collisions, much more limited than the potential LHC yield, indicate that neither conventional parton-showering Monte Carlo generators nor next-to-leading-order QCD calculations are capable of describing forward jet phenomenology. These observations motivate studies of improved methods to compute QCD predictions in the multiple-scale kinematics implied by the forward region.

We have analyzed the high-energy factorization that serves to sum consistently to higher orders in α_s both the logarithmic corrections in the large rapidity interval and those in the hard jet transverse energy. We have determined the gauge-invariant (though not on shell) high-energy amplitudes, which are needed to evaluate the factorization formula for forward jet hadroproduction.

Our results can be used along with $k_\perp$-dependent kernels for parton branching. They can serve to construct predictions for exclusive observables associated to forward jets, including jet correlations, that take into account gluon coherence not only in the collinear emission region but also in the large-angle emission region.

Acknowledgments

One of us (F.H.) visited DESY at various stages while this work was being done and wishes to thank the DESY directorate for hospitality and support. Part of this work was carried out during the 2009 DESY Institute on Parton Showers and Resummations. We thank the organizers and participants in the workshop for the stimulating atmosphere. We gratefully acknowledge useful discussions with S. Baranov, J. Collins, A. Knutsson, A. Lipatov, Z. Nagy, T. Rogers and N. Zotov.

References

[1] CMS collaboration, G.L. Bayatian et al., *CMS physics: Technical Design Report*, CERN-LHCC-2006-001 [SPIRES]; *Jet reconstruction in the CMS Forward Hadron calorimeter in proton-proton collisions at* $\sqrt{s} = 14$ *TeV*, CMS PAS FWD-08-001 (2008).

[2] ATLAS collaboration, P. Jenni et al., *ATLAS Forward Detectors for Measurement of Elastic Scattering and Luminosity*, CERN-LHCC-2008-004; *Zero Degree Calorimeters for ATLAS*, CERN-LHCC-2007-001.

JHEP09(2009)121

[3] FP420 R and D collaboration, M.G. Albrow et al., *The FP420 R&D Project: higgs and New Physics with forward protons at the LHC*, arXiv:0806.0302 [SPIRES].

[4] CMS and TOTEM collaboration, M. Albrow et al., *Prospects for Diffractive and Forward Physics at the LHC*, CERN-LHCC-2006-039 [SPIRES].

[5] X. Aslanoglou et al., *Performance studies of the final prototype for the CASTOR forward calorimeter at the CMS experiment*, CERN-CMS-NOTE-2008-022 [SPIRES]; *Performance Studies of Prototype-II for the CASTOR forward Calorimeter at the CMS Experiment*, *Eur. Phys. J.* **C 52** (2007) 495 [arXiv:0706.2641] [SPIRES].

[6] M. Grothe, *Forward physics with CMS*, arXiv:0901.0998 [SPIRES].

[7] H. Jung et al., *Proceedings of the workshop: hERA and the LHC workshop series on the implications of HERA for LHC physics, 4th workshop on the implications of HERA for LHC*, CERN, Geneva, Switzerland, May 26–30 2008, arXiv:0903.3861 [SPIRES].

[8] A. De Roeck, V.A. Khoze, A.D. Martin, R. Orava and M.G. Ryskin, *Ways to detect a light Higgs boson at the LHC*, *Eur. Phys. J.* **C 25** (2002) 391 [hep-ph/0207042] [SPIRES].

[9] S. Heinemeyer et al., *Studying the MSSM Higgs sector by forward proton tagging at the LHC*, *Eur. Phys. J.* **C 53** (2008) 231 [arXiv:0708.3052] [SPIRES].

[10] D. d'Enterria, *Forward Physics at the LHC: within and beyond the Standard Model*, *AIP Conf. Proc.* **1038** (2008) 95 [arXiv:0806.0883] [SPIRES]; *Low-x QCD physics from RHIC and HERA to the LHC*, *Eur. Phys. J.* **A 31** (2007) 816 [hep-ex/0610061] [SPIRES].

[11] CMS collaboration, S. Cerci and D. d'Enterria, *Low-x QCD studies with forward jets in proton-proton collisions at* $\sqrt{s} = 14$ *TeV in CMS*, *AIP Conf. Proc.* **1105** (2009) 28 [arXiv:0812.2665] [SPIRES].

[12] A. Accardi et al., *Hard probes in heavy ion collisions at the LHC: Jet physics*, CERN-2004-009-B, hep-ph/0310274 [SPIRES]; *Hard probes in heavy ion collisions at the LHC: PDFs, shadowing and pA collisions*, CERN-2004-009-A, hep-ph/0308248 [SPIRES].

[13] CMS collaboration, D.G. d'Enterria, *CMS Physics: Technical Design Report. Volume II: Addendum on High Density QCD with Heavy Ions*, *J. Phys.* **G 34** (2007) 2307 [CERN-LHCC-2007-009] [SPIRES].

[14] A.H. Mueller and H. Navelet, *An Inclusive Minijet Cross-Section and the Bare Pomeron in QCD*, *Nucl. Phys.* **B 282** (1987) 727 [SPIRES].

[15] V. Del Duca, M.E. Peskin and W.-K. Tang, *Computation of mini-jet inclusive cross-sections*, *Phys. Lett.* **B 306** (1993) 151 [hep-ph/9303237] [SPIRES].

[16] W.J. Stirling, *Production of jet pairs at large relative rapidity in hadron hadron collisions as a probe of the perturbative Pomeron*, *Nucl. Phys.* **B 423** (1994) 56 [hep-ph/9401266] [SPIRES].

[17] C. Ewerz, L.H. Orr, W.J. Stirling and B.R. Webber, *BFKL dynamics at hadron colliders*, *J. Phys.* **G 26** (2000) 696 [hep-ph/9912469] [SPIRES];
J.R. Forshaw, A. Sabio Vera and B.R. Webber, *Final states in small x deep inelastic scattering*, *J. Phys.* **G 25** (1999) 1511 [hep-ph/9812318] [SPIRES].

[18] L.H. Orr and W.J. Stirling, *BFKL physics in dijet production at the LHC*, *Phys. Lett.* **B 436** (1998) 372 [hep-ph/9806371] [SPIRES].

[19] J.R. Andersen et al., *Forward jets and forward W boson production at hadron colliders*, hep-ph/0109019 [SPIRES];

JHEP09(2009)121

J.R. Andersen, V. Del Duca, S. Frixione, C.R. Schmidt and W.J. Stirling, *Mueller-Navelet jets at hadron colliders*, *JHEP* **02** (2001) 007 [hep-ph/0101180] [SPIRES].

[20] J.R. Andersen, *All-Order Corrections To Higgs Boson Production In Association With Jets*, arXiv:0906.1965 [SPIRES];
J.R. Andersen and C.D. White, *A New Framework for Multijet Predictions and its application to Higgs Boson production at the LHC*, *Phys. Rev.* **D 78** (2008) 051501 [arXiv:0802.2858] [SPIRES];
J.R. Andersen and A. Sabio Vera, *Solving the BFKL equation in the next-to-leading approximation*, *Phys. Lett.* **B 567** (2003) 116 [hep-ph/0305236] [SPIRES].

[21] A.H. Mueller, *Parton distributions at very small x values*, *Nucl. Phys.* **B** *Proc. Suppl.* **18** (1991) 125 [SPIRES].

[22] W.-K. Tang, *The Structure function νW_2 of hot spots at HERA*, *Phys. Lett.* **B 278** (1992) 363 [SPIRES];
J. Bartels, A. de Roeck and M. Loewe, *Measurement of hot spots inside the proton at HERA and LEP/LHC*, *Z. Phys.* **C 54** (1992) 635 [SPIRES];
J. Kwiecinski, A.D. Martin and P.J. Sutton, *Deep inelastic events containing a measured jet as a probe of QCD behavior at small x*, *Phys. Rev.* **D 46** (1992) 921 [SPIRES];
S. Catani, M. Ciafaloni and F. Hautmann, *Leptoproduction of heavy flavor at high energies*, *Nucl. Phys.* **B** *Proc. Suppl.* **29** (1992) 182 [SPIRES].

[23] H1 collaboration, A. Aktas et al., *Forward jet production in deep inelastic scattering at HERA*, *Eur. Phys. J.* **C 46** (2006) 27 [hep-ex/0508055] [SPIRES];
ZEUS collaboration, S. Chekanov et al., *Forward jet production in deep inelastic e p scattering and low-x parton dynamics at HERA*, *Phys. Lett.* **B 632** (2006) 13 [hep-ex/0502029] [SPIRES].

[24] B.R. Webber, *Hadronic final states*, in *Proceedings of DIS95*, Paris, France, April 24–28 1995, hep-ph/9510283 [SPIRES].

[25] S. Catani, M. Ciafaloni and F. Hautmann, *High-energy factorization in QCD and minimal subtraction scheme*, *Phys. Lett.* **B 307** (1993) 147 [SPIRES]; *High-energy factorization and small x heavy flavor production*, *Nucl. Phys.* **B 366** (1991) 135 [SPIRES]; *Gluon contributions to small x heavy flavor production*, *Phys. Lett.* **B 242** (1990) 97 [SPIRES].

[26] J. Collins, *Rapidity divergences and valid definitions of parton densities*, PoS(LC2008)028 [arXiv:0808.2665] [SPIRES].

[27] F. Hautmann, *Unintegrated Parton Distributions and Applications to Jet Physics*, *Acta Phys. Polon.* **B 40** (2009) 2139.

[28] T.C. Rogers, *Next-to-Leading Order Hard Scattering Using Fully Unintegrated Parton Distribution Functions*, *Phys. Rev.* **D 78** (2008) 074018 [arXiv:0807.2430] [SPIRES].

[29] F. Hautmann, *Endpoint singularities in unintegrated parton distributions*, *Phys. Lett.* **B 655** (2007) 26 [hep-ph/0702196] [SPIRES].

[30] S. Catani and F. Hautmann, *High-energy factorization and small x deep inelastic scattering beyond leading order*, *Nucl. Phys.* **B 427** (1994) 475 [hep-ph/9405388] [SPIRES]; *Quark anomalous dimensions at small x*, *Phys. Lett.* **B 315** (1993) 157 [SPIRES].

[31] V.S. Fadin and L.N. Lipatov, *BFKL Pomeron in the next-to-leading approximation*, *Phys. Lett.* **B 429** (1998) 127 [hep-ph/9802290] [SPIRES];
M. Ciafaloni and G. Camici, *Energy scale(s) and next-to-leading BFKL equation*, *Phys. Lett.* **B 430** (1998) 349 [hep-ph/9803389] [SPIRES].

JHEP09(2009)121

[32] M. Ciafaloni, *Energy scale and coherence effects in small-x equations*, *Phys. Lett.* **B 429** (1998) 363 [hep-ph/9801322] [SPIRES].

[33] F. Schwennsen, *Phenomenology of jet physics in the BFKL formalism at NLO*, hep-ph/0703198 [SPIRES];
J. Bartels, A. Sabio Vera and F. Schwennsen, *NLO jet production in k_T factorization*, arXiv:0709.3249 [SPIRES];
J. Bartels, D. Colferai and G.P. Vacca, *The NLO jet vertex for Mueller-Navelet and forward jets: the gluon part*, *Eur. Phys. J.* **C 29** (2003) 235 [hep-ph/0206290] [SPIRES]; *The NLO jet vertex for Mueller-Navelet and forward jets: the quark part*, *Eur. Phys. J.* **C 24** (2002) 83 [hep-ph/0112283] [SPIRES].

[34] S. Jadach and M. Skrzypek, *QCD evolution in the fully unintegrated form*, arXiv:0905.1399 [SPIRES].

[35] F. Hautmann and H. Jung, *Angular correlations in multi-jet final states from $kt_\perp$-dependent parton showers*, *JHEP* **10** (2008) 113 [arXiv:0805.1049] [SPIRES]; *Three-jet DIS final states from kt-dependent parton showers*, arXiv:0804.1746 [SPIRES].

[36] I. Balitsky, *High-energy effective action from scattering of QCD shock waves*, *Phys. Rev.* **D 72** (2005) 074027 [hep-ph/0507237] [SPIRES].

[37] Y.L. Dokshitzer and G. Marchesini, *Soft gluons at large angles in hadron collisions*, *JHEP* **01** (2006) 007 [hep-ph/0509078] [SPIRES].

[38] Y.L. Dokshitzer, V.A. Khoze, S.I. Troian and A.H. Mueller, *QCD Coherence in High-Energy Reactions*, *Rev. Mod. Phys.* **60** (1988) 373 [SPIRES];
M. Ciafaloni, in *Perturbative Quantum Chromodynamics*, A.H. Mueller ed., World Scientific, Singapore (1989).

[39] Small x collaboration, J.R. Andersen et al., *Small x Phenomenology: summary of the 3rd Lund Small x Workshop in 2004*, *Eur. Phys. J.* **C 48** (2006) 53 [hep-ph/0604189] [SPIRES].

[40] M. Deak, F. Hautmann and H. Jung and K. Kutak, in preparation.

[41] J.C. Collins, *QCD and diffraction*, in Proceedings of *9th International Workshop on Deep Inelastic Scattering (DIS 2001)*, Bologna, Italy, April 27 – May 1 2001, hep-ph/0106126 [SPIRES].

[42] A. Sabio Vera and F. Schwennsen, *The azimuthal decorrelation of jets widely separated in rapidity as a test of the BFKL kernel*, *Nucl. Phys.* **B 776** (2007) 170 [hep-ph/0702158] [SPIRES];
C. Marquet and C. Royon, *Azimuthal decorrelation of Mueller-Navelet jets at the Tevatron and the LHC*, *Phys. Rev.* **D 79** (2009) 034028 [arXiv:0704.3409] [SPIRES];
P. Aurenche, R. Basu and M. Fontannaz, *Jet-jet and hadron-jet correlations in hadro- and electro- production*, *Eur. Phys. J.* **C 57** (2008) 681 [arXiv:0807.2133] [SPIRES];
M. Fontannaz, *Dijet azimuthal correlations in hadron-hadron collisions at high energy*, LPT-Orsay preprint (April 2009).

[43] J.C. Collins and F. Hautmann, *Soft gluons and gauge-invariant subtractions in NLO parton-shower Monte Carlo event generators*, *JHEP* **03** (2001) 016 [hep-ph/0009286] [SPIRES]; *Infrared divergences and non-lightlike eikonal lines in Sudakov processes*, *Phys. Lett.* **B 472** (2000) 129 [hep-ph/9908467] [SPIRES].

[44] E. Iancu, M.S. Kugeratski and D.N. Triantafyllopoulos, *Geometric Scaling in Mueller-Navelet Jets*, *Nucl. Phys.* **A 808** (2008) 95 [arXiv:0802.0343] [SPIRES];

JHEP09(2009)121

Y. Hatta, E. Iancu and A.H. Mueller, *Deep inelastic scattering at strong coupling from gauge/string duality: the saturation line*, *JHEP* **01** (2008) 026 [arXiv:0710.2148] [SPIRES];
E. Iancu, C. Marquet and G. Soyez, *Forward gluon production in hadron hadron scattering with Pomeron loops*, *Nucl. Phys.* **A 780** (2006) 52 [hep-ph/0605174] [SPIRES];
C. Marquet and R.B. Peschanski, *Testing saturation at hadron colliders*, *Phys. Lett.* **B 587** (2004) 201 [hep-ph/0312261] [SPIRES].

JHEP09(2009)121